

# Contrast structure and EDLC performances of activated spherical carbons with medium and large surface areas

Satoshi Mitani<sup>a</sup>, Sang-Ick Lee<sup>b</sup>, Koji Saito<sup>c</sup>,  
Yozo Korai<sup>a,\*</sup>, Isao Mochida<sup>a,1</sup>

<sup>a</sup> Institute for Material Chemistry and Engineering, Kyushu University, Kasuga 816-8580, Fukuoka, Japan

<sup>b</sup> GS Caltex Corporation, 104-4 Munji-Dong, Yusung-Gu, Daejeon-City 305-380, South Korea

<sup>c</sup> Advanced Technology Research Laboratories, Nippon Steel Corporation, 20-1 Shintomi, Futtsu-City, Chiba 293-8511, Japan

Received 7 October 2005; received in revised form 15 February 2006; accepted 22 February 2006

Available online 24 April 2006

## Abstract

Two spherical carbons of 500 and 3000 m<sup>2</sup>/g, respectively, activated with NaOH (M500) and KOH (M3000), were examined in relation to their carbon structure and electrochemical behavior to explain their contrast capacitances as EDLC electrode.

M500 and M3000 showed capacitances per weight (F/g) and volume (F/ml) of 35 and 35 (M500), 40 and 25 (M3000), respectively. The charge profile of M500 by *galvanostat* charge indicated that the charge took place rapidly below 1.5 V and then very gradually increased up to the final voltage of 2.7 V in the first charge. Such electrochemical behavior suggests electric field activation of this particular activated carbon at the charge. The charge profile of M3000 was conventional. The structure of M500 suffered a certain marked expansion at the charge, however the 002 diffractions profile shifted very slightly to a lower angle at the change. Such charge appears reversible while the structure of expansion was more or less irreversible. No expansion was observed with M3000 at the charge to the same voltage.

Such a structure allows high efficiency of EDLC due to small pores and electric field activation to induce small pores among the graphitic units. In contrast, M3000 with its larger surface areas of relatively large pores in the graphitic structure showed a larger capacitance per weight. However many useless pores cause lower the capacitance per volume. In addition, large pores lose the efficiency for the formation of an electric double layer per unit surface area of the pore, while the non-graphitic wall of M3000 fails to introduce small pores with a higher capacitance.

© 2006 Elsevier Ltd. All rights reserved.

**Keywords:** Activated carbon; EDLC; Organic electrolyte; Electric field activation; Cyclic voltammetry

## 1. Introduction

The electric double-layer capacitor (EDLC), using activated carbon as electrode, has been recognized as an efficient storage device for electric power because of its better rate capability and longer life cycle compared to secondary batteries in spite of its low energy density [1,2]. Recently new applications utilizing these properties have been attempted as an energy device for electric or pulse-current supply. In order to meet the specification for new applications, it is necessary to develop a particular activated carbon with much higher energy densities per both

weight and volume than those of the conventional types at large power densities.

Activated carbons with large specific surface areas beyond 2000 m<sup>2</sup>/g have been prepared from various carbon precursors by chemical or gas-phase activation, resulting in fairly high capacitance per weight [3–5]. Nevertheless, they still suffer from low electrode density and capacitance per volume due to a large volume of useless pores as described in a previous paper [6]. The efficiency per surface area even reduced by increasing the surface area beyond 1500 m<sup>2</sup>/g [6], with a less effective surface being inevitably introduced. Hence it is strongly preferable to clarify the key structural factors that govern the super capacitance of activated carbon. The wall surface of the pore with the correct size is a conceptual factor. A too small a pore cannot accept the electrolyte at an acceptable rate, whereas a too large a pore induces useless a void into the carbon body

\* Corresponding author. Tel.: +81 92 583 7800; fax: +81 92 583 7798.

E-mail address: [korai@cm.kyushu-u.ac.jp](mailto:korai@cm.kyushu-u.ac.jp) (Y. Korai).

<sup>1</sup> ISE member.

[7]. Furthermore, too much unadsorbed electrolytes in the pore must reduce the polarity of an adsorbed one through dynamic exchanges. The graphitic structure of the pore wall can also be influential on the efficiency of capacitance. It has been claimed that the edge of the hexagon provides a more effective surface than the basal plane [8–11]. The graphitizable carbon has been reported to show higher capacitance than the non-graphitizable carbon with a similar surface area [12]. The present authors have reported that anisotropic spherical carbons with surface areas of 500 and 2000 m<sup>2</sup>/g being activated with NaOH or KOH of the similar amounts, showed 35 F/g or 35 F/ml and 42 F/g or 18 F/ml, in spite of the same precursor carbon. Such contrast performances of the carbons motivated us to study their structure and electrochemical behaviors in detail.

In the present paper, a structural and electrochemical study was performed on anisotropic spherical carbons activated with NaOH or KOH, in terms of their pore and graphitic structure by BET, Xe NMR, XRD and SEM, as well as their EDLC performances by cyclic voltammetry and charge profile.

## 2. Experimental

### 2.1. Preparation of activated carbon

Optically anisotropic spherical carbon (average particle size: 25  $\mu$ m, quinoline soluble: 5%) prepared from coal-based isotropic pitch was activated with 4 $\times$  NaOH (M500) and KOH (M3000) in weight at 700 °C or 800 °C for 1 h, respectively. The obtained activated carbons (M500 and M3000) showed the specific BET surface areas of 500 m<sup>2</sup>/g (M500) and 3000 m<sup>2</sup>/g (M3000). Details on the preparation of the activated carbons were described in a previous paper [13].

### 2.2. Galvanostat and cyclic voltammetry

The electrode (about 25 mg) was a roll-pressed disc (density: 0.96 g/ml) prepared from a mixture of M500 or M3000, carbon black conductor (Ketjen-black E) and polytetrafluoroethylene (PTFE) binder (8:1:1 weight ratio). The specific capacitance was measured by the two-electrode system using tetraethylammonium tetrafluoroborate (Et<sub>4</sub>NBF<sub>4</sub>: 1 M) in propylenecarbonate (PC) as an electrolyte. The test cell was charged to 2.7 V at a constant current (100 mA/g) and voltage, and then discharged at a constant current (2.4 mA or 2.12 mA/cm<sup>2</sup>) to 0 V. The charge was kept at 2.7 V in the first cycle while the current decreased to 0.3 mA (0.27 mA/cm<sup>2</sup>), for not longer than 80 min, to obtain sufficient charge by the electric field activation.

The specific capacitance was calculated by the following equation:

$$C = \frac{I(T_2 - T_1)}{(V_1 - V_2)(X)}$$

where  $V_1$  and  $V_2$  are 2.16 and 1.08 V, respectively,  $I$  is 2.4 mA and  $X$  is the weight or volume of the two electrodes.

Cyclic voltammetry (CV) was carried out in a typical three-electrode test cell, using 1 M tetraethylammonium tetrafluoroborate (TEATFB) in propylene carbonate (PC) as an electrolyte.

Ag/Ag<sup>+</sup> in acetonitrile and disc-shaped electrode with twice the weight of the working electrode were used as reference and counter electrode, respectively. CV was performed using a potentiostat (Hokudo Denko, Model HA3000) at a scan rate of 3 mV/s in the range of  $-1.7$  to  $1.3$  V (versus Ag/Ag<sup>+</sup>).

### 2.3. Analyses of activated carbons

Morphologies of the activated carbons were observed under a high resolution scanning electron microscope (SEM, JSM-6320, JEOL). X-ray powder diffraction (XRD) of the activated carbons was performed using Cu K $\alpha$  radiation ( $\lambda = 1.54$  Å).

Surface area and pore size distribution of the activated carbons were measured according to the BET method by physical adsorption of N<sub>2</sub> at  $-196$  °C, using an automatic adsorption system (FISONS INSTRUMENTS SORPTOMATIC 1990). Hyper-polarized <sup>129</sup>Xe gas was prepared through laser-aided polarization apparatus (Toyoko Kagaku Co., Japan), which contacted Rb waper with Xe gas under the irradiation of the laser near the external magnet [14]. The polarized <sup>129</sup>Xe gas (10 ml) was introduced via a plastic syringe into a 10 mm-size glass NMR tube containing the sample carbons. A <sup>129</sup>Xe NMR spectrum was obtained using <sup>129</sup>Xe gas without any adsorbent (0 ppm) as external standard. The activated carbon was degassed overnight at 150 °C under vacuum before <sup>129</sup>Xe NMR measurement. The average pore size of a particular carbon was obtained by comparing its chemical shift in its <sup>129</sup>Xe NMR on the master curve as reported previously [14,15].

## 3. Results

### 3.1. SEM appearances and average pore sizes of activated carbons

Fig. 1 shows N<sub>2</sub> absorption isotherms and pore size distributions of M500 and M3000. Fig. 1(a) shows typical adsorption isotherms. In case of Fig. 1(b), both carbons have pores around 1 nm although their pore volumes and surface areas were very different. Fig. 2 shows SEM photographs of M500 and M3000. M500 stayed fairly graphitic after NaOH activation, whereas M3000 lost graphitic structure by KOH activation. M500 showed a rather smooth surface, while M3000 showed a very rough surface with a numbers of pores, which reflected its very large surface area.

<sup>129</sup>Xe NMR spectra of M500 and M3000 with specific surface areas of 500 and 3000 m<sup>2</sup>/g are shown in Fig. 3. The spectra showed a sharp peak at 0 ppm and a rather broad one at the higher magnetic field. A sharp and a broad peak can be assigned to the non-absorbed <sup>129</sup>Xe on the outer surface and the adsorbed <sup>129</sup>Xe in the pore of the carbon, respectively. Chemical shifts of the adsorbed <sup>129</sup>Xe on the pore wall of M500 and M3000 were found to be 100 and 60 ppm, respectively. The average pore sizes of M500 and M3000 obtained by comparing their chemical shifts on the master curve were noted as 0.97 and 1.6 nm. The intensity of the adsorbed Xe may reflect its amount in the pore and hence the pore volume.

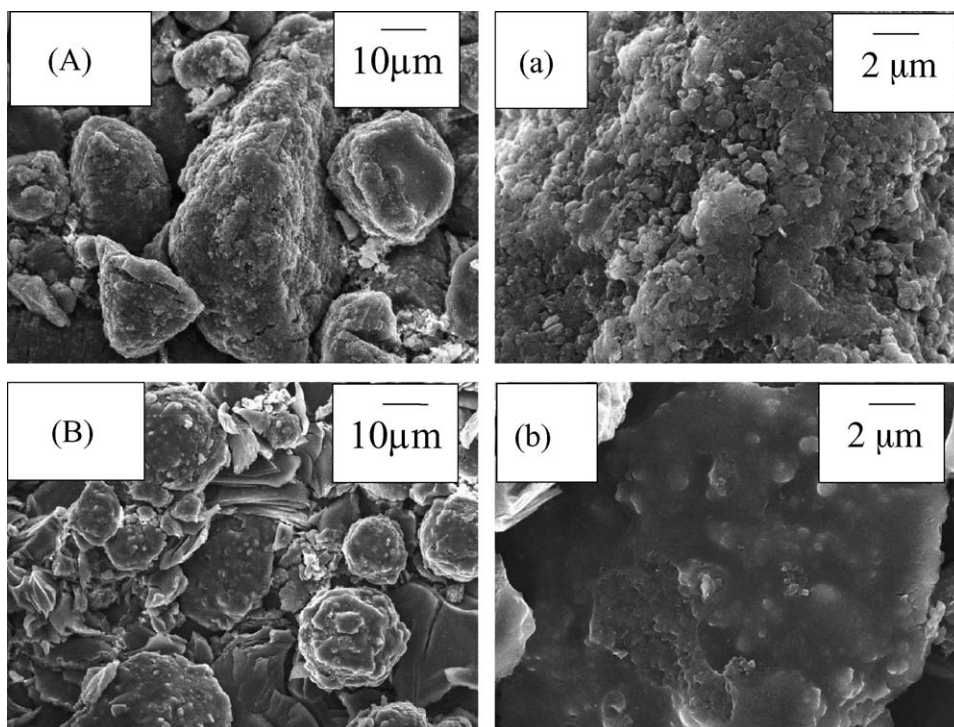
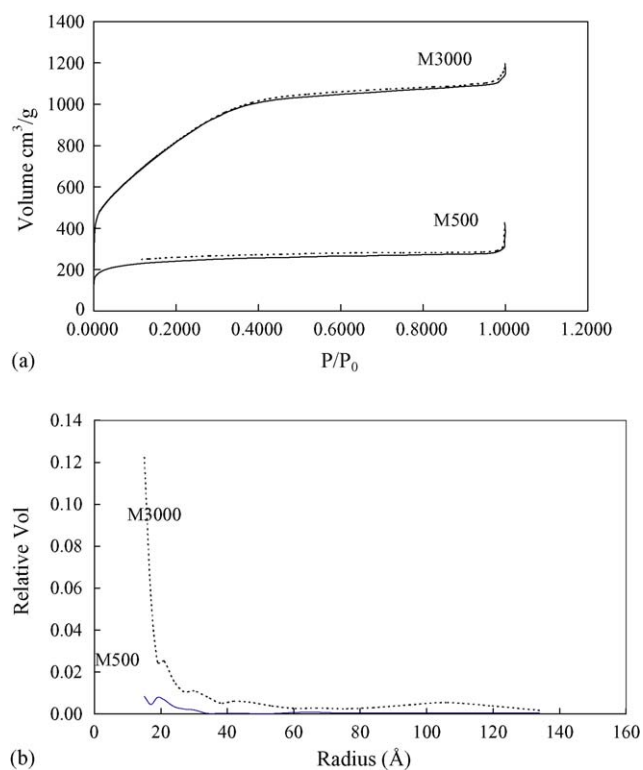
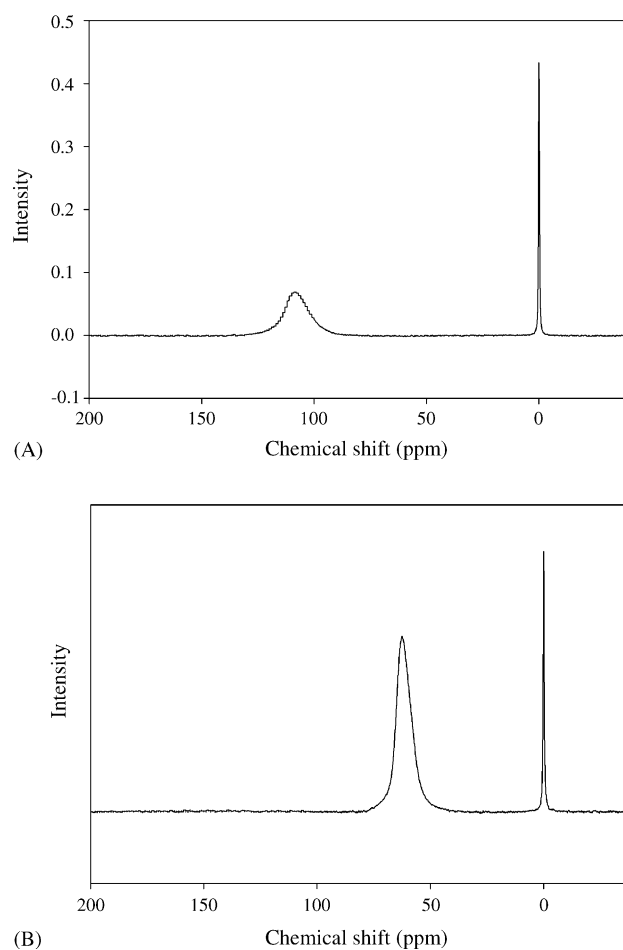


Fig. 1. SEM image of M500 (A, a) and M3000 (B, b).

Fig. 2. Adsorption isotherm (a) and pore size distribution (b) over M500 and M3000. According to N<sub>2</sub> adsorption at 77 K.Fig. 3. <sup>159</sup>Xe NMR spectra over M500 (A) and M3000 (B).

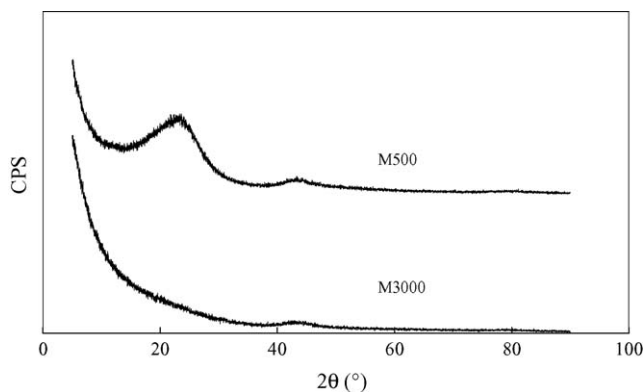


Fig. 4. XRD of activated spherical carbons of M500 and M3000.

### 3.2. Graphitic structure of M500 and M3000

Fig. 4 illustrates the XRD of activated spherical carbons of M500 and M3000. M500 maintained a definite 0 0 2 diffraction although it was very broad, whereas M3000 hardly showed any diffraction. The graphitic structure must survive in M500 during NaOH activation to obtain 500 m<sup>2</sup>/g, whereas KOH activation lost the graphitic structure while M3000 obtained 3000 m<sup>2</sup>/g.

### 3.3. Charge behaviors and cyclic voltammetry of M500 and M3000

Fig. 5 shows charge profiles of M500 and M3000 to 2.7 V. The very contrasting profiles are illustrated in Fig. 5. M500 showed

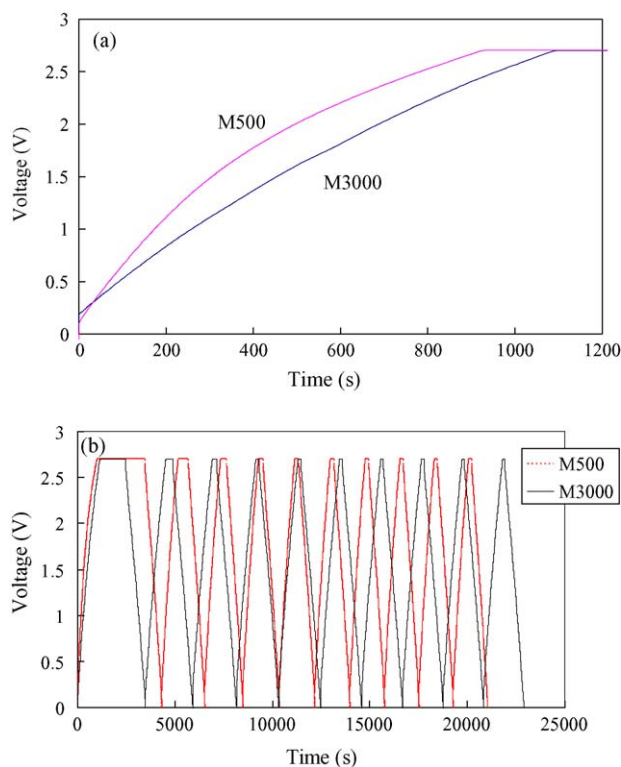


Fig. 5. Charge and discharge profiles of M500 and M3000. (a) First cycle of charge; (b) 10 cycles of charge and discharge.

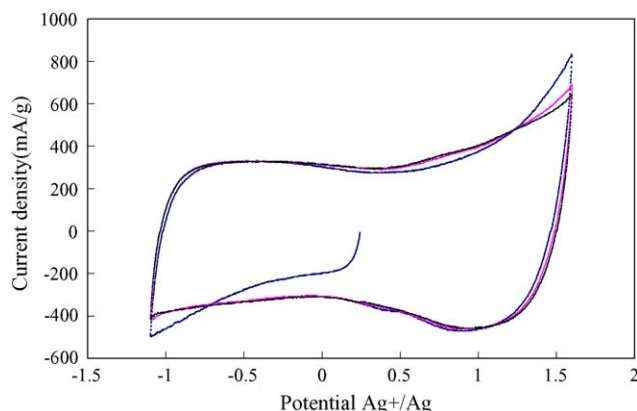


Fig. 6. Cyclic voltammogram of M500 at the sweep scan rate of 3 mV/s.

a rapid increase of charge voltage within 300 s to achieve 2 V and then very gradually increased above 2 V, to reach 2.7 V. In contrast, M3000 showed a steady increase of voltage over time. A linear increase of voltage over time indicates a proportional increase of adsorption with an increase of the charge voltage. The gradual increase may indicate the change in pore structure of M500 at charges above 2 V.

The potential sweep cyclic voltammograms of M500 and M3000 are illustrated in Figs. 6 and 7. The first cycle profile of M500 showed a gradual increase of the current density at 0–1.1 V, and a sharp increase of current density to –500 mA/g at the anode of –1.1 V, and 800 mA/g at the cathode of 1.5 V. The unsymmetrical and non-rectangular shape showed different current densities at the positive and the negative electrodes. The repeated cycle removed the gradual increase and reduced the sharp increases both at –1.1 and 1.5 V, becoming a conventional profile from cycle to cycle.

In contrast, the cyclic voltammogram of M3000 in Fig. 7 shows a typical rectangular shape, although there was a slight increase of the current density by the charge at 1.5 V. The typical rectangular shape has been often observed with conventional activated carbon. The capacitances of the positive and negative electrodes of M500 on the three-electrode cell were calculated at 33.3 and 25 F/g, respectively, based on the respective current

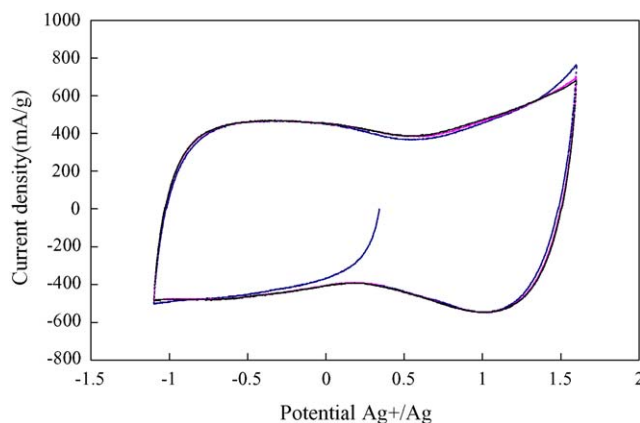


Fig. 7. Cyclic voltammogram of M3000 at the sweep rate of 3 mV/s.



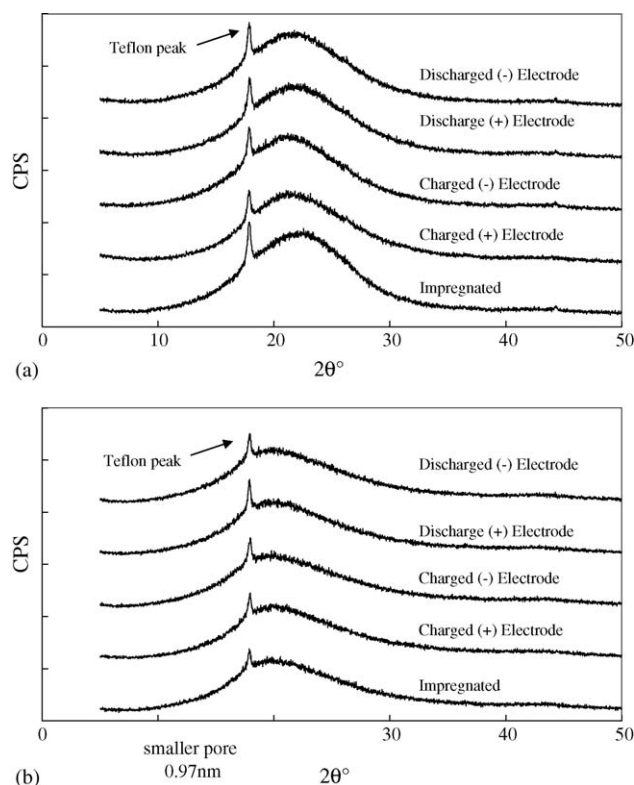


Fig. 8. (a) XRD pattern of electrode (M500) after charge and discharge. (b) XRD pattern of electrode (M3000) after charge and discharge.

density at the positive and negative electrodes by the following equation:

$$\text{Capacitance of two electrode cell} = \frac{\text{CV (current density) [mA/g]} \times \frac{1}{4}}{\text{Scan rate [mV/s]}} \times \frac{1}{4} \quad (1)$$

↑  
Capacitance of three electrode cell

The larger capacitance of the positive electrode than negative electrode is shown with M500 by charge at 1.5 and  $-1.1$  V, respectively.

### 3.4. XRD of activated carbons after charge and discharge

Fig. 8 illustrates the XRD of M500 and M3000 electrodes in the impregnated, charged and discharged stages at 2.7 V. Impregnation to both carbons markedly decreased the diffraction below the  $10^\circ$  enhanced 002 diffraction in comparison to the as-prepared carbons. The charge shifted and slightly broadened the 002 line of M500 at both positive and negative electrodes. Discharge recovered the 002 line at both electrodes. The 002 line of the much less-graphitic M3000 changed hardly in shape and position by impregnation, charge and discharge. Little structural change of M3000 is therefore suggested due to electrochemical forces.

Table 1

Deformation of electrode after charge and discharge at 3.7 V

Stage	SA ( $\text{m}^2/\text{g}$ )	Pore volume ( $\text{m}^3/\text{g}$ )
M3000		
Impregnation	1913	1.18
Positive	1643	0.97
Negative	1329	0.76
M500		
Impregnation	123	0.17
Positive	273	0.24
Negative	209	0.22

### 3.5. Surface area and pore volume of activated carbons after charge and discharge

Table 1 summarizes the surface area and pore volume of the M500 and M3000 electrodes in the impregnated, charged and discharged stages. These electrodes were charged at 3.7 V in order to clarify deformation of structure carbon under electric field activation. Their surface area of M3000 measured by  $\text{N}_2$  adsorption–desorption ranged from  $1329 \text{ m}^2/\text{g}$  (negative) and  $1643 \text{ m}^2/\text{g}$  (positive), to  $1913 \text{ m}^2/\text{g}$  (impregnation). The surface area of M500 ranged from  $123 \text{ m}^2/\text{g}$  (impregnation) and  $273 \text{ m}^2/\text{g}$  (positive), to  $209 \text{ m}^2/\text{g}$  (negative). Their pore volume depended on the surface area. The pore volume of M3000 ranged from  $0.76 \text{ m}^3/\text{g}$  (negative) to  $1.18 \text{ m}^3/\text{g}$  (impregnation). On the other hand, the pore volume of M500 ranged from  $0.17 \text{ m}^3/\text{g}$  (impregnation) to  $0.24 \text{ m}^3/\text{g}$  (positive).

## 4. Discussion

### 4.1. Behavior of $\text{Et}_4\text{NBF}_4$ electrolyte in PC in the electrode

The electrolyte dissolved in the polar PC solvent penetrates into the pore of the activated carbon electrode with the solvent molecule in the capacitor when the electrode is impregnated into the electrolyte solution. Both ions of the electrolyte can behave separately or in their ion pair form to penetrate the pore. A portion of the electrolyte can be adsorbed in forms of ion pairs or the dissociated cation and anion on the carbon wall of the pore. The polar solvent can be also adsorbed onto the wall itself.

The results in Table 1 clearly suggest behaviors of the  $\text{Et}_4\text{NBF}_4$  electrolyte in PC in the electrode. The surface area of the M3000 electrode in the impregnated stage is larger than after charge and discharge (positive or negative stage). With activated carbon, including a number of micro pores such as M3000, it was assumed that some of the electrolytes cannot depart the micro pore because of the strong interaction with the pore wall.

While comparing the before charge and discharge (impregnation stage) with the after charge and discharge (positive or negative stage), the surface area of the electrode after the charge and discharge is higher than before the charge and discharge.

It was assumed that deformation of the structure was caused under electric field conditions.

The electric field under the charge enhances the penetration and the adsorption of the electrolytes or its dissociated ions in the more polarized state, to form the electric double layer over

the surface of the pore wall, storing electric energy as the capacitor. At this stage, the electrolyte or its particular ion moves into or out of the pore in the electrode according to their charges to enhance the adsorption in the double layer under the electric field. A higher electric force can allow the penetration of an electrolyte ion into the very narrow void where the electrolyte cannot be present without an electric field, increasing the capacitance of the carbon according to the charged stage. Such an increase can reversibly or irreversibly change the micro porosity of the carbon. This kind of capacitance increase under the field is depending on the electric field activation of the carbon [12,15].

The discharge desorbs the adsorbed species to reduce the thickness of the double layer, releasing the electric energy stored on the carbon surface.

Hence, there are several states of the electrolyte or its ions present dissolved in the electrolyte solvent at the charged and discharged, as well as impregnated stages. There are also several kinds of pores in terms of size and shape as well as of wall structures in terms of graphitic extent, surface carbon arrangement, and functional groups. There should be a significant correlation between the structure and the state of the electrolyte solution over the activated carbon surface which governs the EDLC performance as discussed in the present study.

#### 4.2. The penetration of the electrolyte into the pores

The average diameters of the pore in the present M500 and M3000 activated carbons were estimated to be 0.97 and 1.59 nm as suggested by Xe NMR. According to *ab initio* molecular orbital calculation by Ue et al. [16], the cation ( $\text{Et}_4\text{N}^+$ ) and the anion ( $\text{BF}_4^-$ ) of the electrolyte in the present study have respective solvated sizes of 0.68 and 0.44 nm in propylene carbonate. The simple sum of both ions corresponding to the size of their ion pair is estimated to be 1.12 nm, which is certainly larger than the average pore diameter of M500. Hence, the cation and

the anion in the polar solvent must separately penetrate into the pores, while the same numbers of both ions are present in the pore, ruling out a strong pairing at their penetration in the particular polar solvent.

#### 4.3. Electrochemical origin for high EDLC of M500

Volumetric capacitance of M500 was definitely larger than that of M3000 as illustrated in Figs. 3 and 4 in spite of the much smaller surface area of M500. The larger capacitance per surface area of M500 is ascribed partly to the significant increase of its capacity between 0.5 and 2.0 V in the positive electrode, and non-negligible one at  $-1.5$  V in the negative electrode. Such an increase with M500 was also indicated by the charge profile in Fig. 5 where the sharp increase of charge voltage above 2.7 V was observed exclusively in the first charge. In comparison with M3000, significant enhancement in the activated penetrations or adsorption of the electrolyte ions must take place at such relatively high voltages at both electrodes of M500 (especially the positive electrode), significantly increasing its capacitance. M500 can be a typical case of such an activation. The extent of such an activation appears to strongly depend on the detailed structure of the carbon, leading to the irreversible change of its pore. It is often observed at this stage that the carbon tends to expand its volume by charge at higher voltages. The penetration of the electrolyte is suggested into the voids under the charge, expanding the narrow voids. Such a structural change can be favorable to give higher capacitance in a certain voltage range by increasing the effective surface area of the electrode carbon.

The size of such an induced pore can be defined to take most effective size to the maximum capacitance per volume by the electrolyte size pushed into the carbon void.

In addition to such an activation, M500 showed a comparable capacitance at its rectangular part of the cyclic voltammetry in Fig. 6 in spite of its significantly smaller surface area compared to M3000. This fact may indicate a higher efficiency in

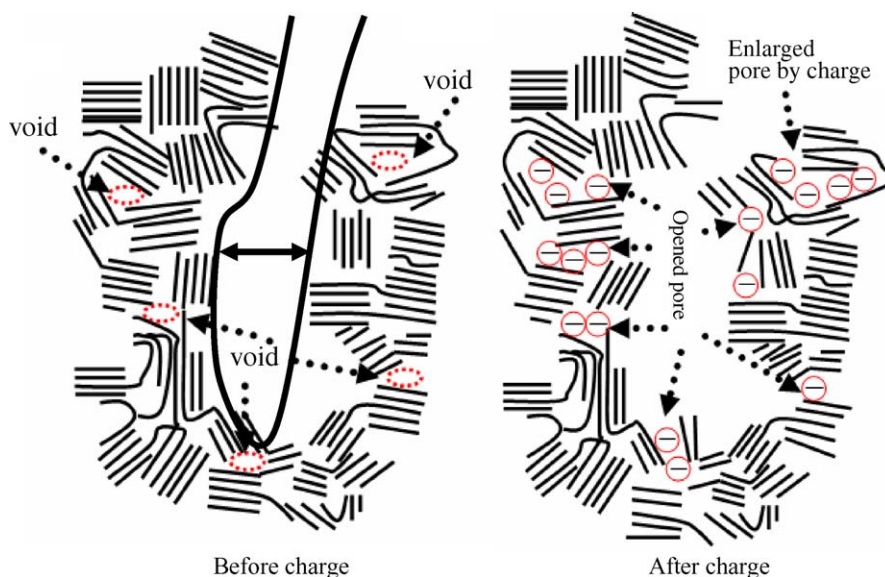


Fig. 9. Structure image of M500.

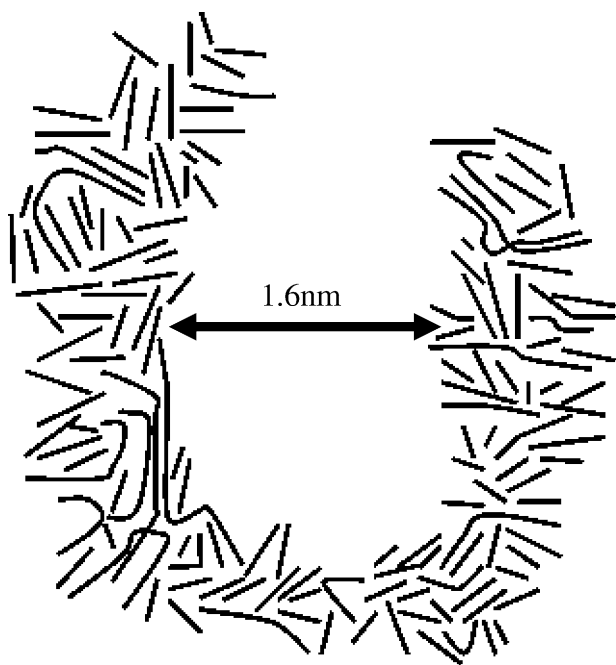


Fig. 10. Structure image of M3000.

the polarization of the ion over the wall surface of the smaller pores in M500. Average diameter of pores in M500 is certainly smaller than that of M3000. Smaller diameter of pores included a lesser amount of non-adsorbed electrolyte or its ion, leading to a smaller exchange between adsorbed and non-adsorbed ones in the same pore. A smaller exchange may keep the polarization extent of adsorbed species high to be favorable for the capacitance per unit surface area.

It must be also emphasized that the electric field activation can occur only within the very small void in the carbon where the electrolyte is forced to penetrate exclusively under the electric field. No significant intercalation of the electrolyte takes place between stacking layers of grapheme sheets. The higher polarization of the electric double layer is expected in the smaller pore, because high density of the charge on the wall of the small pore must be compensated with the solvated electrolyte ions of high polarization.

#### 4.4. Structural characteristic of M500 leading to larger capacitance per surface area

The structure characteristics of M500 are smaller pores in lesser numbers and highly graphitic pore walls. The advantage

of the former feature was described above. The graphitic wall has two aspects related to its performances of capacitance. The edge and basal planes of the carbon hexagon have been reported to show very different activity for the EDLC [8–11]. The more graphitic wall may have more chance to expose the hexagon edge of thickness and width in the graphitic units on the wall surface, being favorable for a higher capacitance.

Figs. 9 and 10 illustrate images of M500 and M3000 structures, respectively. The graphitic wall of M500 must consist of graphitic clusters. The electrode or its ion can penetrate into the narrow voids among clusters under a high electric field to expand the size accessible to the ions.

The opened void can be most the effective pore for high capacitance. On the other hand, the graphitic structure of M3000 was broken almost completely by KOH activation, and hence the narrow void did not exit. Thus, the graphitic structure is favorable for such activation. This can be an important advantage of M500. The effective charge voltage must be high because of the high electric conductivity due to highly graphitic structure. This is also another advantage of M500.

#### References

- [1] A. Nishino, J. Power Sources 60 (1996) 137.
- [2] T. Christen, M.W. Carlen, J. Power Sources 91 (2000) 210.
- [3] H. Teng, Y. Chang, C. Hsieh, Carbon 39 (2001) 1981.
- [4] M. Endo, T. Maeda, T. Takeda, Y.J. Kim, K. Koshiba, H. Hara, M.S. Dresselhaus, J. Electrochem. Soc. 148 (2001) A910.
- [5] A. Nishino, K. Naoi, Technologies and Materials for EDLC and Electrochemical Supercapacitors, CMC, Tokyo, 2003, pp. 129–174.
- [6] S. Mitani, S.-I. Lee, S.-H. Yoon, Y. Korai, I. Mochida, J. Power Sources 133 (2004) 298.
- [7] I. Tanahashi, A. Yoshida, A. Nishino, Bull. Chem. Soc. Jpn. 63 (1990) 3611.
- [8] H.H. Bauer, M.S. Spritzer, P.J. Elving, J. Electroanal. Chem. 17 (1968) 299.
- [9] J.P. Randin, E. Yeager, J. Electrochem. Soc. 118 (1971) 711.
- [10] J.P. Randin, E. Yeager, J. Electroanal. Chem. 36 (1972) 257.
- [11] J.P. Randin, E. Yeager, Electroanal. Chem. Interfacial Electrochem. 58 (1975) 313.
- [12] M. Takeuchi, T. Maruyama, K. Koike, A. Mogami, T. Oyama, H. Kobayashi, Electrochemistry 69 (2001) 487.
- [13] S.-I. Lee, S. Mitani, S.-H. Yoon, Y. Korai, I. Mochida, Carbon 42 (2004) 2332.
- [14] K. Saito, A. Kimura, H. Fujiwara, Magn. Reson. Imaging 21 (2003) 401.
- [15] S. Mitani, S.-I. Lee, K. Saito, S.-H. Yoon, Y. Korai, I. Mochida, Carbon 43 (2005) 2960.
- [16] M. Ue, A. Murakami, S. Nakamura, J. Electrochem. Soc. 149 (2002) A1385.